INTEGRATED DESIGN AND RAPID DEVELOPMENT OF REFRACTORY METAL BASED ALLOYS FOR FOSSIL ENERGY APPLICATIONS

Michael C. Gao
U.S. DOE National Energy Technology Laboratory
1450 Queen Ave SW, Albany, OR 97321
Parsons, P.O. Box 618, South Park, PA 15129

Wren Chan
Department of Materials Science and Engineering, Carnegie Mellon University,
5000 Forbes Ave, Pittsburgh, PA 15289

Ömer N. Doğan
U.S. DOE National Energy Technology Laboratory
1450 Queen Ave SW, Albany, OR 97321
Phone: 541-967-5858; Fax: 541-967-5845; email: omer.dogan@netl.doe.gov

Paul King
U.S. DOE National Energy Technology Laboratory
1450 Queen Ave SW, Albany, OR 97321

ABSTRACT

In order to develop ductile Cr-based structural alloys that also have good creep resistance and corrosion resistance for advanced fossil power generation technologies at ultra-high temperatures, we have adopted an integrated approach that utilizes the multi-scale computational methods to design materials for requirements of processing and performance. This report summarizes our accomplishments in FY 2009, which includes mechanical property prediction using first principles calculations, and computational thermodynamic modeling using CALPHAD method.

INTRODUCTION

Modern technologies (e.g. oxy-fuel gas turbines, hydrogen turbines) for fossil power generation systems require new materials that can withstand ultra-high temperatures (Turbine blade substrate metal temperatures are predicted to be 1450°C for oxy-fuel turbines, and 1175°C for hydrogen turbines) and aggressive environments (e.g., steam, oxygen, CO, etc.). Owing to its relatively low cost, the relatively low density and good high temperature strength, we have selected Cr to demonstrate that integrated design methodology works well in developing new high temperature materials based on refractory metals. In order to improve the ductility and fracture toughness of Cr at room temperature, we have used first principles density functional theory (DFT) calculations to guide alloying strategies[1]. In addition, excellent oxidation resistance of Cr alloys must be extended to higher temperatures and improved creep strength must be achieved.

Our approach is to develop theoretical modeling to guide experimental alloy development to avoid traditional trial-and-error experiments that are also time consuming and expensive. Such theoretical modeling can be multiscale in nature, which include first principles DFT calculations, and atomistic, mesoscale and continuum simulations. Previously we studied the alloying effect of 24 potential elements on structural, electronic, elastic and thermodynamic properties of binary $Cr_{15}X_1$ alloys , including Ti, V, Mn, Fe, Co, Ni, Zr, Nb, Mo, Tc, Ru, Rh, Pd, Hf, Ta, W, Re, Os, Ir, Pt, Al, Si, Ga, Ge and vacancy[1]. We chose Poisson's ratio as the screening parameter because an alloy tend to more ductile if it has a high Poisson ratio[2, 3]. Based on that, we have identified several feasible alloying elements that act as potent ductilizing addictives for further theoretical investigation. These elements are Fe, Ti, Zr, Hf, V, Nb, Mo and Ta.

In this report, we have extended our DFT study into ternary and higher-order system alloys. How the structural, electronic, elastic and thermodynamic properties of Cr alloys will change with various combinations of these elements in compositions has been studied theoretically. The goal of such computations is to identify compositions that are very ductile, possess high melting point, and high strength with coherent strengthening second-phase particles. In order to develop a self-consistent thermodynamic database for Cr alloys, we have optimized several Cr-based binary phase diagrams.

FIRST PRINCIPLES CALCULATIONS

The first principles package of VASP (Vienna *ab initio* simulation package) [4, 5] was used in this study which solves for the electronic band structure using electronic density functional theory. Projector augmented-wave [6] pseudopotentials are used as supplied with VASP. The Perdew-Burke-Ernzerhof [7] gradient approximation to the exchange-correlation functional was used. Brillouin zone integrations were performed using the Monkhorst–Pack k-point meshes [8], and a smearing parameter of 0.2 eV was chosen for the Methfessel–Paxton [9] technique.

Reciprocal space (k-point) meshes are increased to achieve convergence to a precision of better than 1 meV/at. All structures are fully relaxed (both lattice parameters and atomic coordinates) until energies converge to a precision of 1 meV/at. A "high precision" setting is used. The plane-wave energy cutoff is held constant at 500 eV. The semi-core 3p, 4p and 5p electrons of transition elements are explicitly treated as valence. Electronic spin polarization with collinear magnetization or anti-ferromagnetism is considered in all calculations since Cr is known as anti-ferromagnetic at its ground state [1]. The calculated atomic magnetic spin moment is ±1.211 Bohr magnetons for pure Cr.

To calculate the single crystal elastic constants, the stress-strain approach outlined in Ref. [10] is used. After full relaxation of each composition, a series of small strain at δ=±0.005, ±0.01, ±0.015, ±0.02, ±0.025 is applied to the crystal with the volume fixed. The elastic constants are then extracted from a linear least-square fit of the first-principles Hellmann–Feynman stresses calculated at those applied strains. The isotropic polycrystalline bulk modulus (B) and shear modulus (G) are taken from the average of theoretical lower and upper bounds of B and G respectively given by Reuss (assuming uniform stress throughout polycrystalline solid) and Voigt (assuming uniform strain) [10], i.e. $B = (B_R + B_V)/2$; $G = (G_R + G_V)/2$. The quantities of B_R, B_V, G_R and G_V (see the equations presented in Ref. [10]) can be computed from the elastic compliances, which are obtained through the inversion of the elastic constant matrix.

Among all the elements in the periodic table, three elements exhibit extensive solid solutioning with Cr based on published binary phase diagrams [11], namely V, Fe and Mo (see Figure 1), therefore, they are selected as major alloying elements. V is the only element that can form complete bcc solid solutioning with Cr over the whole temperature range. At high temperatures, Fe and Cr forms complete bcc solid solutioning, however, a topological closed packed (TCP) phase forms at intermediate temperatures followed by a sluggish miscibility gap at lower temperatures. For Cr-Fe based multicomponent alloys studied by Brady et al.[12] neither this TCP phase not miscibility gap was reported, demonstrating that their stability may be only limited to the terminal binary. On the other hand, Mo and Cr forms complete bcc solid solutioning at high temperatures, however, there exists a wide miscibility gap at lower temperatures. Whether this miscibility gap could be depressed in multicomponent system is not known at this stage.

The calculated Poisson's ratio for CrV-, CrFe- and CrMo-based ternary alloys are presented in Figure 2. The exact compositions are not disclosed for confidentiality purpose. There are several ternary CrV alloys that are predicted to have a Poisson's ratio of above 0.40, implying that intrinsically they are very ductile. A few CrFe and CrMo ternary alloys also show potentially strong ductility enhancement. However, caution should be paid to the hypothesis we made here: (1) we assume all the ternary compositions examined have a bcc structure, but in reality they may not exist because of phase stability issue. This is mainly due to the fact that there are few Cr-based ternary phase diagrams available in the literature; (2) we only examine one atomic configuration for each composition, but there may be various configurations depending on depending on which positions the solute atoms are assigned to. Nevertheless, the calculations from the present study offer instructive guidance on which elements and to what extent we should design our experimental efforts.

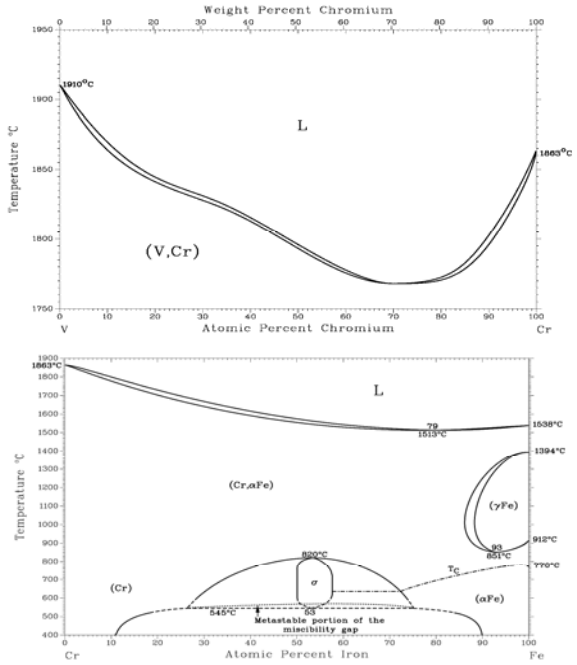

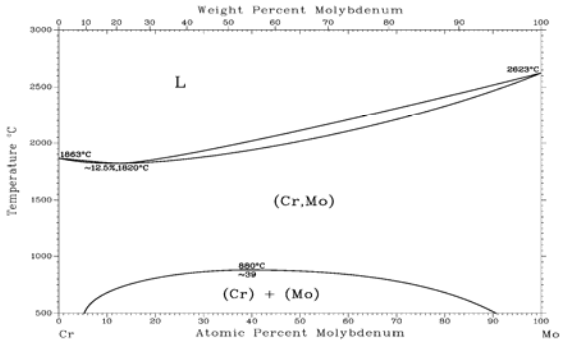

Figure 1: Published Cr-V, Cr-Fe and Cr-Mo binary alloy phase diagrams [11].

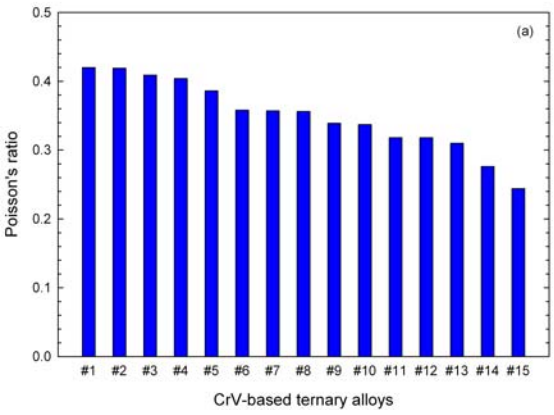

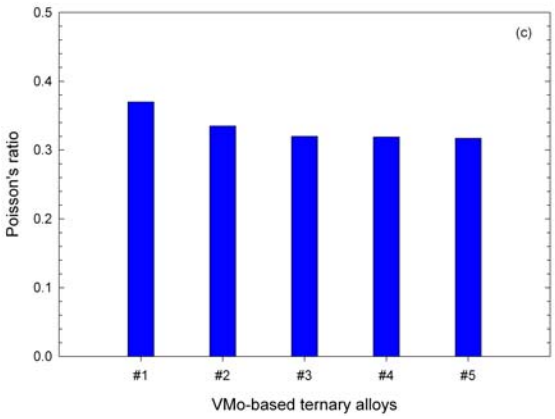

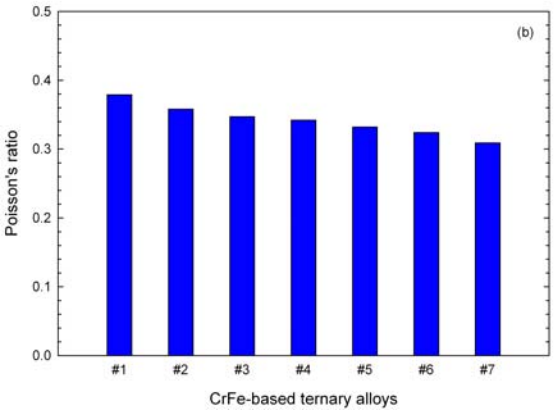

Figure 2: *ab initio* calculated Poisson's ratio for (a) CrV-based, (b) CrFe-base, and (c) CrMo-based ternary alloys. The exact compositions are not disclosed for confidentiality purpose.

THERMODYNAMICS MODELING

Phase diagrams and their inherent thermodynamic properties are the keys to alloy design and process. To achieve the desired function during processing, one requires the best possible knowledge of the relevant phase field and thermodynamic descriptions of all phases. For this purpose, CALPHAD method has been developed substantially in the past several decades, and CALPHAD techniques based on critically evaluated data are widely used as a basic tool in the development and optimization of materials and processes of many different types. Considerable time and cost can be saved in the experimental development work if the calculations involved can be made sufficiently reliable.

In this report, we use Cr-Ce as an example to demonstrate the methodology of CALPAHD modeling in developing thermodynamic database. The terminal phases in Cr-Ce are βCe (dhcp), γCe (fcc), δCe (bcc) and *Cr* (bcc) above room temperature.[13] This system was experimentally studied by Savitskii *et al.*[14] and Kobzenko *et al.*,[15] and the data are largely restricted to Cr-rich solid-liquid equilibrium, the monotectic temperature and composition, and the eutectic temperature. Data from Kobzenko *et al.*[15] show appreciable scatter for both solidus and liquidus lines with temperatures ranging from 1790 to 1820°C. The monotectic temperature is 1780 ± 10°C and composition approximately 95.18 at.% Cr while extent of solubility of Ce in Cr ranges from 0.56-0.75 at.% to 2.72 at.%.[14] The eutectic temperature was determined to be 780°C based on thermal analysis of cerium-rich alloys.[14] The phase diagram provided by Savitskii *et al.*[14] also includes points corresponding to phase stability values of *Cr* and the two phase region (*Cr* + Liquid). The experimental methods reported by Savitskii *et al.*[14] were electronic chromatic pyrometry (for liquidus lines), Pironi's drop method (for solidus lines), photomicroscopy (for solubility) and thermal analysis (for the eutectic point). From 715°C to 785°C, δCe and Cr are relatively immiscible in each other with some solubility of Cr in δCe and little solubility of Ce in Cr. According to Massalski *et al.*[13] a eutectic reaction: Liquid ↔ Cr + δCe occurs at 785°C at around 5 at.% Cr and a eutectoid reaction: δCe ↔ Cr + γCe occurs at 715°C at around 1 at.% Cr.

The Gibbs energy for each element is defined with respect to its stable state at 298.15 K and 1 atm. In the CALPHAD method, the Gibbs energy of pure elements is represented as a power series in terms of temperature in the form:

$$G = a + bT + cT\ln(T) + \sum_n d_n T^n \qquad \text{(Eq. 1)}$$

where a, b, c and dn are coefficients and n represents a set of integers typically of the values of 2, 3 and -1. Typically the thermodynamic data for pure elements are taken from SGTE-Pure v4[16] for database compatibility purpose. However, in this study the data for Cr, La and Y was taken from SGTE-Pure v4[16] and that for Cr was taken from SGTE-SSOL4 v4. The reason is that SGTE-Pure v4[16] treats the polymorphic transformation temperature of γCe ↔ βCe at 10°C while SGTE-SSOL4 v4 treats it at 61°C. The authors think the latter is more appropriate because it is 139°C on heating and -16°C on cooling according to Massalski *et al.*[13] It appears that the SGTE-SSOL4 database takes the average temperature at 61°C. Therefore, future experiment to measure this polymorphic transformation is required to clarify the discrepancy.

The Gibbs energy of individual solid solution phases (e.g. liquid, bcc, fcc, hcp and dhcp) was modeled using the sublattice solution model:

$$G^{\Phi} = x_{Cr}\overline{G}_{Cr}^{\Phi} + x_{Ce}\overline{G}_{Ce}^{\Phi} + G^{id} + G_m^{ex} + G_m^{mag} \qquad \text{(Eq. 2)}$$

$$G^{id} = \mathrm{R}T \cdot \left[x_{Cr}\ln(x_{Cr}) + x_{Ce}\ln(x_{Ce})\right] \qquad \text{(Eq. 3)}$$

$$G_m^{ex} = x_{Cr}x_{Ce} \cdot \sum_{v=0}^{n} {}^{v}L_{Cr,Ce}(x_{Cr} - x_{Ce})^{v} \qquad \text{s} \qquad \text{(Eq. 4)}$$

$${}^{v}L_{Cr,Ce} = a_v + b_v T + c_v T\ln(T) \qquad \text{(Eq. 5)}$$

$\overline{G}_{Cr}^{\Phi}$ and $\overline{G}_{Ce}^{\Phi}$ are the Gibbs energy of the pure elements in the solution phase Φ; G^{id} is the ideal mixing energy; G_m^{ex} is the excess energy of the phase using the Redlich-Kister polynomial form;[17] x_{Cr} and x_{Ce} are the mole fractions of the constituents; ${}^{v}L_{Cr,Ce}$ is the binary interaction parameter of Cr and RE of an order v, R is the gas

constant and T is the absolute temperature (K). G_m^{mag} is the Gibbs energy due to magnetic ordering, but it was set to zero in this study because of lack of experimental data and the fact that terminal solid solutions are truly negligible.

The calculated Cr-Ce binary phase diagram is shown in Fig. 2 with experimental data from solidus and liquidus points.[14] The invariant reactions are listed in Table 2. The Cr-rich liquidus and solidus were determined over a relatively narrow range of temperatures from around the reported melting point (T=1900°C) to the monotectic (T = 1780°C).[14, 15] The calculated compositions of phases at the eutectic and monotectic equilibrium are largely in disagreement with the existing phase diagram[11] though the invariant temperatures are consistent. The calculated values show that the liquid at the monotectic point contains around 15 at.% less Cr than reported.[14] The discrepancy between the calculated liquid composition at the eutectic point and the accepted composition[13] differs by around 4 at.%. A consistent thermodynamic assessment of the Cr-Ce could not be obtained to agree with both temperature and composition at both monotectic and eutectic reaction. However a good fit is obtained with the phase stability data points and liquidus and solidus values on the Cr-rich end as reported.[14] As experimental data that led to the accepted composition[13] is irretrievable, the optimized eutectic composition can be considered an acceptable estimate. Although the monotectic composition is significantly off the reported value,[14] considering the difficulty of high temperature measurement and the difficulty of measuring the monotectic composition directly, the estimate is reasonable as the solidus and liquidus[14] suggest a reasonable fit.

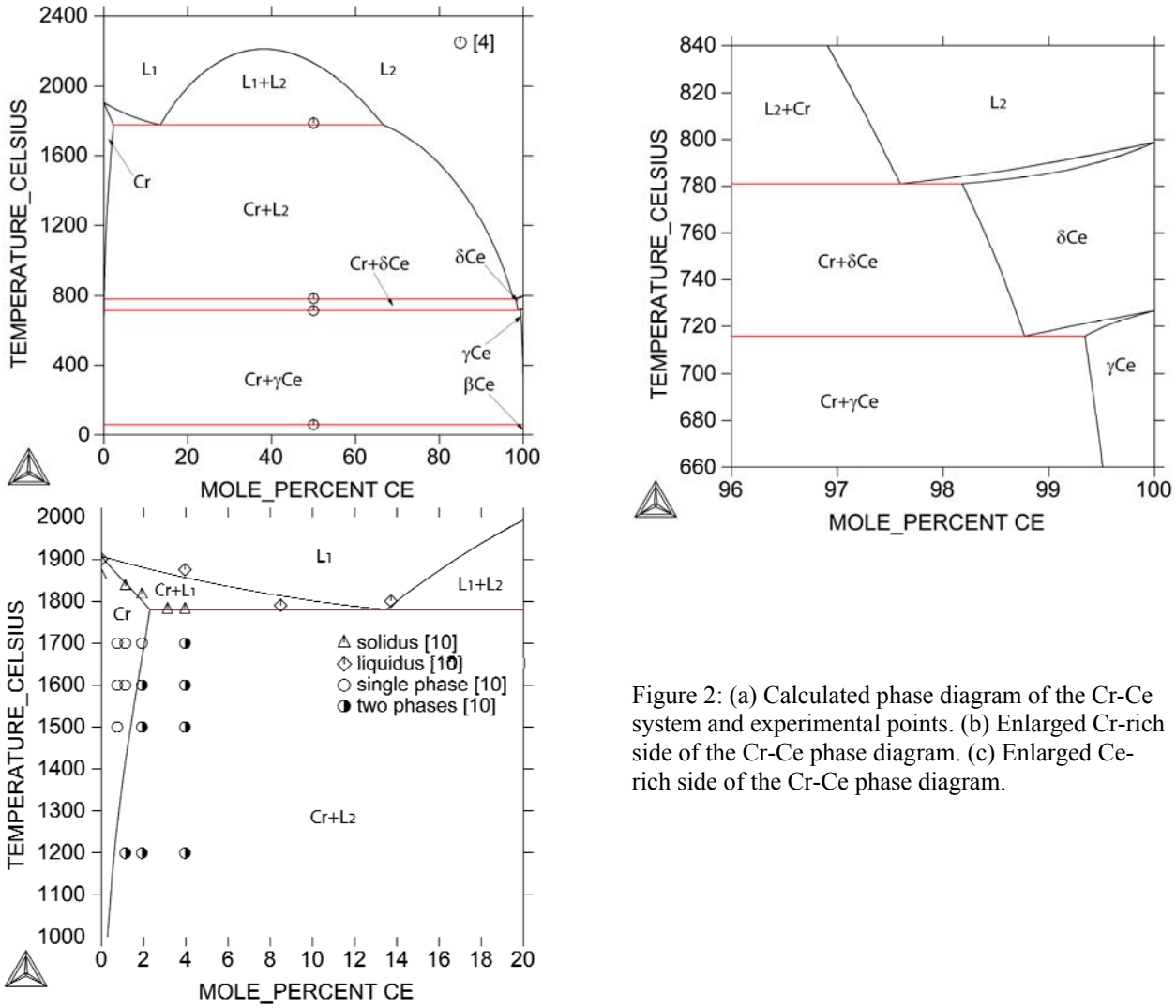

Figure 2: (a) Calculated phase diagram of the Cr-Ce system and experimental points. (b) Enlarged Cr-rich side of the Cr-Ce phase diagram. (c) Enlarged Ce-rich side of the Cr-Ce phase diagram.

CONCLUSIONS

In summary, we have used first principles DFT calculations to screen a large number of CrV-, CrFe- and CrMo-based ternary alloys theoretically for intrinsic ductility enhancement of pure Cr. Several compositions are predicted to have a high value of Poisson's ratio and can be targeted for further theoretical study and experimental verification. We also used Cr-Ce binary system as an example to demonstrate the CALPHAD methodology.

ACKNOWLEDGEMENT

This work was performed in support of the National Energy Technology Laboratory's Strategic Center for Coal under the RDS contract DE-AC26-04NT41817.

REFERENCES

[1] M. C. Gao, Ö. N. Doğan, P. King, A. D. Rollett, and M. Widom, JOM **60**, 61 (2008).
[2] S. F. Pugh, Phil. Mag. **45**, 823 (1954).
[3] A. H. Cottrell, in *Advances in Physical Metallurgy*, edited by J. A. C. a. G. C. Smith (Institute of Metals, London, 1990), p. 181.
[4] G. Kresse and J. Hafner, Phys. Rev. B **47**, 558 (1993).
[5] G. Kresse and J. Furthmueller, Phys. Rev. B **54**, 11169 (1996).
[6] P. E. Blochl, Phys. Rev. B **50**, 17953 (1994).
[7] J. P. Perdew, K. Burke, and M. Ernzerhof, Phys. Rev. Lett. **77**, 3865 (1996).
[8] H. J. Monkhorst and J. D. Pack, Phys. Rev. B **13**, 5188 (1976).
[9] M. Methfessel and A. T. Paxton, Phys. Rev. B **40**, 3616 (1989).
[10] C. Jiang, S. G. Srinivasan, A. Caro, and S. A. Maloy, J. Appl. Phys. **103** (2008).
[11] T. B. Massalski, H. Okamoto, P. R. Subramanian, and L. Kacprzak, *binary alloy phase diagrams* (ASM International, Materials Park, OH 44073, 1995).
[12] M. P. Brady, C. T. Liu, J. H. Zhu, P. F. Tortorelli, and L. R. Walker, Scripta Materialia **52**, 815 (2005).
[13] T. B. Massalski, P. R. Subramanian, H. Okamoto, and L. Kacprzak, *Binary Alloy Phase Diagrams, 2nd ed., vols. 1-3.* (ASM International, Materials Park, OH.
[14] E. M. Savitskii, V. F. Terekhova, and A. V. Kholopov, Russian J. Inorg. Chem. **4**, 195 (1959).
[15] G. F. Kobzenko, A. G. Kholodov, V. G. Ivanchenko, E. L. Martinchuk, and O. N. Kashevskaya, Metallofizika (Russian). **33**, 95 (1971).
[16] A. Dinsdale, CALPHAD **15**, 317 (1991).
[17] O. Redlich and A. T. Kister, Ind. Eng. Chem. **40**, 345 (1948).